The CLIVAR C20C Project: Which components of the Asian-Australian Monsoon circulation variations are forced and reproducible?

Tianjun Zhou[1*], Bo Wu[1, 2], A. A. Scaife[3], S. Brönnimann [4], A. Cherchi[5], D. Fereday[3], A. M. Fischer[4], C. K. Folland[3], K. E. Jin[7], J. Kinter[7], J. R. Knight[3], F. Kucharski[6], S. Kusunoki[9], N.-C. Lau[8], Lijuan Li[1], M. J. Nath[8], T. Nakaegawa[9], A. Navarra[5] ,P. Pegion[10], E. Rozanov[4,11], S. Schubert[10], P. Sporyshev[12], A. Voldoire[13] , Xinyu Wen[14,1], J.H. Yoon[15], N. Zeng[15]

1 LASG, Institute of Atmospheric Physics, Chinese Academy of Sciences, China

2 Graduate University of Chinese Academy of Sciences, China

3 Met Office Hadley Centre, Exeter, UK.

4 Institute for Atmospheric and climate science, ETH, Switzerland

5 Centro Euromediterraneo per i Cambiamenti Climatici, and Istituto Nazionale di Geofisica e Vulcanologia, Bologna, Italy

6 Abdus Salam International Center for Theoretical Physics, Italy

7 Centre for Ocean-Land-Atmosphere studies, USA.

8 Geophysical Fluid Dynamics Laboratory, NOAA, USA.

9 Meteorological Research Institute, Japan Meteorological Agency, Japan

10 NSAS Goddard Space Flight Center, USA.

11 Physical-Meteorological Observatory/World Radiation Center, Switzerland

12 Voeikov Main Geophysical Observatory, Russia

13 CNRM, Meteo France, France

14 Department of Atmospheric Sciences, Beijing University, China

15 University of Maryland, USA

Climate Dynamics

(Revised in Sep 2008)

* Email: zhoutj@lasg.iap.ac.cn

Abstract

A multi-model set of atmospheric simulations forced by historical sea surface temperature (SST) or SSTs plus Greenhouse gases and aerosol forcing agents for the period of 1950-1999 is studied to identify and understand which components of the Asian-Australian monsoon (A-AM) variability are forced and reproducible. The analysis focuses on the summertime monsoon circulations, comparing model results against the observations. The priority of different components of the A-AM circulations in terms of reproducibility is evaluated. Among the subsystems of the wide A-AM, the South Asian monsoon and the Australian monsoon circulations are better reproduced than the others, indicating they are forced and well modeled. The primary driving mechanism comes from the tropical Pacific. The western North Pacific monsoon circulation is also forced and well modeled except with a slightly lower reproducibility due to its delayed response to the eastern tropical Pacific forcing. The simultaneous driving comes from the western Pacific surrounding the maritime continent region. The Indian monsoon circulation has a moderate reproducibility, partly due to its weakened connection to June-July-August SSTs in the equatorial eastern Pacific in recent decades. Among the A-AM subsystems, the East Asian summer monsoon has the lowest reproducibility and is poorly modeled. This is mainly due to the failure of specifying historical SST in capturing the zonal land-sea thermal contrast change across the East Asia. The prescribed tropical Indian Ocean SST changes partly reproduce the meridional wind change over East Asia in several models. For all the A-AM subsystem circulation indices, generally the MME is always the best except for the Indian monsoon and East Asian monsoon circulation indices.

Key words: CLIVAR C20C, Asian-Australian monsoon circulation, AGCM, reproducibility

1. Introduction

One aim of the CLIVAR International "Climate of the 20th Century (C20C)" Project is to test whether climate models are able to reproduce recent climate variations and to find the responsible mechanisms (Folland et al. 2002). The 20th century variability of monsoon climate has been a topic of C20C (e.g., Kucharski et al. 2008). Asian scientists and the public society are always interested in advancing the knowledge of the predictability of summer monsoon, because the economy and society across the region are critically influenced by the evolution and variability of the monsoon. A better prediction of the monsoon variation may greatly benefit the humanity inhabiting the region. Therefore, predictability and variability of the monsoon are active research areas (e.g., Parthasarathy et al. 1991; Webster and Yang 1992; Ju and Slingo 1995; Hu 1997; Chang et al. 2000a,b; Wang 2001; Gong and Ho 2002; Hu et al. 2003; Yu et al. 2004; Wang et al. 2005; Zhou and Yu 2005, 2006; Yang and Lau 2006; Yu and Zhou 2007; among many others).

Previous studies showed difficulties in simulating or predicting the Asian-Australian monsoon (A-AM) precipitation. Most of these previous studies used Atmospheric General Circulation Models (AGCMs) where the SST anomalies were prescribed. The poor performance of forecasts/simulations is attributed to the large internal variability of the monsoon with weak control from local boundary forcing factors (Krishnamurti et al. 2006). An early study indicated that the precipitation variations over India for the period 1979-88 are not well simulated by

AMIP (Atmospheric Model Inter-comparison Project) models, partly due to the errors in the mean states of the models (Sperber and Palmer 1996). Examinations on the tropical precipitation anomalies associated with the 1997/98 El Nino showed that most of the AGCMs have difficulty in simulating the negative precipitation anomalies over the Maritime Continent (Kang et al. 2002). Analysis of multi-model ensemble two-tier prediction system found that the signal-to-noise ratio of seasonal mean precipitation over the monsoon region is lower than that of other tropical regions (Kang and Shukla 2006). When prescribed by SST forcing, the AGCM simulated anomalous summer precipitation in the A-AM region has a pattern correlation considerably poorer than its counterpart in the tropical central-eastern Pacific region (Wang et al. 2004). This is partly due to the neglect of air-sea coupling in AMIP-type simulations. Recent studies suggested that the A-AM simulation depends on the correct air-sea coupling (Wang et al. 2005; Wu and Kirtman 2005; Wu et al. 2006).

The ability of models' simulation of interannual variability may also have a close link to its fidelity of climate mean state simulation (Fennessy et al. 1994). Bias of climate models in the mean state and the seasonal cycle could compromise the skill of seasonal and interannual predictability (Gadgil and Sajani 1998; Sperber et al. 2001). Analysis of multi-model ensemble two-tier prediction system found all models produce large systematic errors in the Asian monsoon region, particularly in the western Pacific. As a result, all models exhibit very poor correlation skill over the monsoon region. The multi-model ensemble prediction does not improve the

correlation skill (Kang and Shukla 2006). An improvement in ocean-atmosphere coupled model's mean state could generally lead to a realistic simulation of ENSO-monsoon teleconnection (Lau and Nath 2000; Turner et al. 2005). A comparison between AMIP-type and coupled model experiments suggested that in a coupled model SST biases may interfere with the benefits deriving from an active air-sea coupling (Cherchi and Navarra 2007). Great advances have been made in recent years in the filed of model improvements. A recent analysis on the output of AMIP II models, which was run in an AGCM-alone way forced by historical sea surface temperature covering the period 1981-2002, shows that the multi-model ensemble simulation of the seasonal precipitation anomalies captures the first two leading modes of the interannual variability of A-AM with a skill that is comparable to the reanalysis in terms of the seasonally evolving spatial patterns and the corresponding interannual variations, as well as their relationships with ENSO (Zhou et al. 2008a). Recent examinations of changes in global monsoon precipitation over land revealed an overall weakening over the recent half century (Wang and Ding 2006; Zhou et al. 2008b). This significant change is deducible from the atmospheric model's response to specified historical SSTs, although the skill over the A-AM domain is far from satisfaction due to either the neglect of air-sea coupling or errors in the mean state of the model (Zhou et al. 2008c). These results suggested that at least part of the monsoon precipitation variability is reproducible from atmospheric response to prescribed SST forcing. In addition, a recent analysis on C20C outputs indicated that whereas on the interannual timescale

there is only a modest skill in producing the precipitation variability over the South Asian domain (70°E-95°E, 10°N-30°N), on decadal timescale the skill is much larger (Kucharski et al. 2008).

The A-AM domain, spanning from about 40ºE to 160ºE and from 30ºS to 40ºN, covers one-third of the global tropics and subtropics (Wang 2006). The A-AM system is comprised of several sub-monsoon components, e.g. the Indian monsoon, the Australian monsoon, the western North Pacific monsoon, and the East Asian monsoon. In previous studies the predictability or reproducibility of monsoon is generally discussed by analyzing precipitation over the entire A-AM domain, which could downplay the tropical and subtropical difference of predictability or reproducibility. In addition, previous analyses primarily focused on precipitation. Precipitation is not only the most important but also most difficult variable for climate prediction (Wang et al. 2005; Kang and Shukla 2006) or climate mean state simulation (Zhou and Li 2002). Examination of precipitation prediction is the most rigorous test for climate models. Only focusing on precipitation might overlook the potential predictability of monsoon circulation. A study of atmospheric circulation variations is an essential pre-requisite for understanding precipitation variations. There are evidences suggesting the reproducibility of major circulation anomalies associated with the interannual variations of the A-AM (Li et al. 2005, 2006), and its subsystems (Cherchi and Navarra 2003). The present study tries to separate different parts of A-AM system that hopefully bear respective predictability or reproducibility in their variations. We focus on large or regional scale dynamic

fluctuations rather than on the regional-scale precipitation variations. We investigate which components of the A-AM circulation variation can be reproduced in atmospheric models with prescribed SSTs and radiative forcing agents using a multi-model inter-comparison performed in the context of the CLIVAR International C20C Project (Folland et al. 2002). Our results indicate that the South Asian monsoon measured by means of a broad-scale circulation index is generally better reproduced than the others. The order of reproducibility for the circulations of A-AM subsystems in the context of correlations between the observed and simulated indices is as follows: the Australian monsoon, the Western North Pacific monsoon, the Indian monsoon, and the East Asian monsoon.

The rest of the paper is organized as follows. Section 2 briefly describes the model, the methodology and the datasets used. Section 3 examines whether the observed variability of different A-AM components can be captured by the C20C simulations, along with a discussion on the forcing mechanism in Section 4. Section 5 summarizes the study and its findings.

2. Models, data and analysis method

The models that have been examined in this study include 12 AGCMs from the C20C project participants. In addition to the models from the C20C partners, we have also finished a global SST-forced 12-member ensemble simulations at LASG/IAP by using the National Center for Atmospheric Research (NCAR) CAM 2.0.1 model (Zhou and Yu 2006). Thus we have the outputs of 13 models. Table 1 shows a brief

summary of each model. The twentieth-century climate AGCM simulations were made with combinations of forcing agents including the observed SSTs and sea-ice extents from the HadISST data set (Rayner et al. 2003), greenhouse gases (GHGs), sulfate aerosols, stratospheric aerosols due to volcanic eruptions, stratospheric and tropospheric ozone, and solar irradiance changes. A description of the integrations is provided on the C20C website (http://www.iges.org/c20c). References of the models are also listed in Scaife et al. (2008). The documentation of the NCAR CAM2 model is provided in Collins et al. (2003). The model simulations cover the period 1870-2002, or subsets of it. Ensemble simulations are performed and many models have more than one realization. Our analysis focuses on the last 50 years of the 20th century, i.e. 1950-1999, a period having relatively solid observational data for model evaluations.

The following data are used for model evaluation: (1) The sea level pressure (SLP), 850 hPa and 200 hPa wind fields from the National Center for Environmental Prediction–National Center for Atmospheric Research (NCEP henceforth) reanalysis data covering 1950 to 1999 (Kalnay et al. 1996); (2) The observational SST data obtained from the Hadley Centre sea ice and sea surface temperature (HadISST) analyses (Rayner et al. 2003). In addition, we have also used the ERA40 reanalysis data (Uppala et al. 2005) to evaluate the model results and the conclusions are nearly the same, which give further fidelity to the results reported here. For brevity, we only show the results based on the NCEP reanalysis. Note in the following discussions, all the correlation/regression analyses and the trend calculations are done for the

1950-1999 period.

The reproducibility of A-AM variability is assessed by computing the correlation coefficients between the observed and simulated monsoon circulation indices. There are large regional differences in the circulation anomalies in the A-AM domain. Following Wang et al. (2001, 2004), to facilitate the assessment of the models' performance on regional monsoon variability, several dynamic monsoon indices are used for each monsoon subsystem:

(1) The Webster-Yang index (WYI), which is defined as the vertical zonal wind shear between 200 and 850 hPa (U850-U200) averaged over the South Asian region (0°-20°N,40°-110°E) to measure the broad-scale South Asian summer (JJA) monsoon circulation anomalies (Webster and Yang 1992);

(2) The Indian summer (JJA) monsoon index (IMI), which is defined as the meridional differences of the 850 hPa zonal winds averaged over the domains (5°-15°N,40°-80°E) and (20°-30°N,60°-90°E), that is,

IMI=U850(5°-15°N,40°-80°E)-U850(20°-30°N,60°-90°E)

The IMI essentially depicts the vorticity of the Indian monsoon trough and associated southwesterly monsoon. The IMI is highly correlated with the all-Indian precipitation index (Wang et al. 2001).

(3) The western North Pacific summer monsoon index (WNPMI), which is defined as the meridional differences of the JJA 850 hPa zonal winds averaged over the domains (5°-15°N, 100°-130°E) and (20°-30°N, 110°-140°E), that is,

WNPMI=U850(5°-15°N, 100°-130°E)-U850(20°-30°N, 110°-140°E)

The WNPMI depicts the vorticity of the western North Pacific (WNP) monsoon trough and associated southwesterly monsoon. The WNPMI is highly correlated with the dominant leading mode of 850 hPa winds over the WNP (Wang et al. 2001).

(4) The Australian summer monsoon index (AUSMI), which is defined as the DJF 850 hPa zonal wind anomalies averaged over 0°-10°S, 120°-150°E. Since the Australian summer monsoon is characterized by the presence of equatorial westerlies at 850 hPa overlaid by equatorial easterlies at 200 hPa (McBride 1987), this circulation index is proposed to measure the low-level monsoon flows (Wang et al. 2004).

(5) The East Asian summer monsoon index (EASM hereinafter), which is defined as the summation of JJA SLP difference (ΔSLP) between 110°E and 160°E from 10°N to 50°N. This is a traditional index used in quantifying the East Asian monsoon variability (Guo 1983). The ΔSLP shows the pressure gradient between land (110°E) and sea (160°E). Negative value indicates that the wind is mainly directed from south to north. Integrating the ΔSLP emphasizes general intensity of summer monsoon. The notion behind this definition is that the east-west land-sea thermal contrast determines the southerly monsoon strength over the East Asia. We term this index as East Asian monsoon SLP index in the following discussion.

In addition, since both the east-west and north-south thermal contrasts dominate the East Asian summer monsoon (Zhu et al. 2005), a more straightforward measure of

the monsoon intensity is the meridional wind over the East Asian domain. We employ another monsoon index here as the average of JJA 850 hPa meridional wind over the region (20°-45°N, 110°-120°E) (Wang 2001). This index is termed as East Asian monsoon meridional wind index in the following discussion.

The IMI, WNPMI, AUSMI, and EASM provide succinct descriptions of the four major subsystems of the A-AM, while WYI measures the broad-scale South Asian monsoon circulation. Our strategy for deciding whether atmospheric models are capable of reproducing prominent events from the observational climate record follows that posed by Scaife et al. (2008):

(1) To identify which events can be reproduced given radiative forcing agents and observational sea surface conditions, we first compare ensemble means of simulations with the observations. A good resemblance of the simulation to the observation indicates that these events are "***forced***".

(2) If the observational response is outside the range of ensemble mean model responses, we then compare the observations with the ensemble members to determine if the event has occurred by chance due to internal atmospheric variability. If so, these events are "***unforced but reproducible***". If the observations are outside the range of both the ensemble mean and the ensemble spread, we say these events are "***poorly modeled***".

3. Results

In this section, we show the time series of various monsoon indices in Figure 1, along with a comparison of the standard deviations of different monsoon index time series derived from the reanalysis and multi-model simulations in Figure 2. The correlation coefficients between the observation and the simulation for different monsoon indices are shown in Figure 3. To reveal the internal variability, correlation coefficients between the monsoon indices derived from each realizations of ensemble simulation and the observation are shown in Figure 4. Figure 5 shows the trends of different monsoon indices from 1950 to 1999 derived from the observations and simulations. To reveal the internal variability, similar trends as Figure 5 except for each realization are shown in Figure 6. To facilitate the discussions on monsoon - ENSO relation, regressions of monsoon index upon the Nino-3 index (a regional average of sea surface temperature within 150°W-90°W and 5°N-5°S) are given in Figure 7. In the following analysis, according to the strategy described in section 2, we first compare the ensemble simulation with the observation to see whether the monsoon variations are forced. If the correlation is low, we further examine the role of internal variability. The long-term trends of different monsoon indices are also examined in this way.

a) South Asian monsoon

We first examine the performance of multi-model ensemble (MME) simulation of the broad-scale South Asian monsoon circulation, which is measured in terms of the Webster-Yang index. The modeled Webster-Yang index time series is shown in

Figure1a against that derived from the reanalysis. The strengths of inter-annual variability, measured by the standard deviation (*std*), simulated by different models are different (Figure 2). This is mainly due to the spread among model sensitivities. Note the *std* of MME simulation is generally weaker than the observation for all monsoon indices (Figure 2). This is expected since working with ensemble always increases the correlation but decreases the amplitude, as random variations are reduced during the averaging (Zhou and Yu 2006). To facilitate the display of model results paralleling the reanalysis, the normalized rather than actual time series are used throughout the paper. The Webster-Yang index derived from the reanalysis shows robust interannual fluctuations. This interannual variation is quite well reproduced in the MME simulation, having a correlation coefficient of 0.65 with the reanalysis (Figure 3), which exceeds the 5% level of statistical significance. There are spreads among the models; however, most models (12 out of 13) show reasonable skills, as evidenced by the statistically significant correlation coefficients at the 5% level given in Figure 3. Note a correlation coefficient larger than 0.28 is considered as statistically significant at the 5% level. The low skill of ARPEGE model is partly due to the disturbance of internal noise, because this model only has one realization (Figure 4a). Thus in terms of MME mean, the observed variation of the South Asian monsoon quantified by the Webster-Yang index is potentially reproducible, forced and well modeled. The MME is always the best index in comparison with that derived from individual models. The reproducibility is driven by the tropical Pacific forcing (Figure 7a).

The reanalysis shows that the South Asian monsoon has been weakening at a rate of -0.89 per 50 yrs (Figure 5a), which is statistically significant at the 10% level. The trend of MME mean is -1.34 per 50 yrs, which is statistically significant at the 5% level (Figure 5a). Wang et al. (2004) showed that the Seoul National University AGCM composite of five runs failed to reproduce this trend, suggesting the model-dependence of their results. This difference also emphasizes the necessity of employing MME (Figure 5a) or ensemble simulation (Figure 6a). However, our results do not demonstrate that all the C20C models are perfect in reproducing this weakening tendency. In fact, half models overestimate while half models underestimate the observational trend (Figure 5a).

b) Indian monsoon

The Indian monsoon index shows a lack of significant trend or climate change signal but contains multi-decadal variation (Figure 1b). From Figure 5b, the trend is only about -0.25/50yr, which is not statistically significant at the 5% level. The decade between 1950 and 1960 exhibited more above normal monsoon, while the decade between 1980 and 2000 exhibited more below normal monsoon. This epochal variation of Indian summer monsoon has been stated in many previous studies (e.g., Parthasarathy et al. 1991). Both the year-to-year and epochal changes are partly reproduced by the MME simulation. The correlation between the reanalysis and the MME is 0.32 (Figure 3), which is lower than that of the Webster-Yang index but still statistically significant at the 5% level. Most models

show skills lower than the MME. The relatively low skills of individual models may be resulted from the disturbance of internal noise (Figure 4). It is worth mentioning that some models are better than the MME. This indicates that the MME may not always be the best index as is often the case. In addition, although the monsoon-ENSO connection has been weakening in recent decades as to be discussed in Section 4, the monsoon-ENSO relationship is still significant in the statistics (Figure 7b).

c) Western North Pacific monsoon

The interannual variability of the western North Pacific monsoon is well reproduced in the MME (Figure 1c), having a correlation coefficient of 0.45 with the reanalysis, which is statistically significant at the 5% level, and lower (higher) than the Webster-Yang index (Indian monsoon index) (Figure 3). Most models, 7 out of 13, have statistically significant correlations with the reanalysis at the 5% level (Figure 3). Both the HadAM3 and GFDL models show relatively better results. The spread among different realizations are also similar in these two models (Figure 4). The index derived from the MME is always the best or at least comparable to the best model.

The western North Pacific monsoon does not show any trend in the reanalysis (Figure 5). Most models, 10 out of 13, show positive trends, and 3 of them are statistically significant at the 5% level. There are also two models showing negative trends (Figure 5c). The MME mean shows a weak positive trend, which is not

statistically significant at the 5% level. The spreads among different realizations are large, indicating the disturbance of internal noise (Figure 6c). This is also true for the other monsoon indices.

In addition, the remote El Nino or tropical Pacific forcing only has a weak simultaneous contribution to the interannual variability of the western North Pacific monsoon (Figure 7c). The responses of the western North Pacific monsoon to tropical Pacific forcing are stronger than the reanalysis in most models, as indicated by the significant regressions shown in Figure 7c. As will be discussed in Section 4, since the western North Pacific monsoon has a 6-months lagged response to El Nino forcing during the El Nino decaying summer (Li and Wang 2005), the simultaneous driving of SSTA here comes from the western Pacific surrounding the Maritime Continent. In the WNP region, ECHAM4 simulates a better summer monsoon precipitation distribution when coupled with a dynamical ocean model than when forced with prescribed SST, highlighting the importance of air-sea coupling in this region (Cherchi and Navarra 2007).

d) Australian monsoon

The Australian monsoon exhibits a strong interannual variability in the reanalysis (Figure 1d). This year-to-year variation is well reproduced in the MME mean (Figure 3), having a correlation coefficient of 0.59 with the reanalysis, which is statistically significant at the 5% level except slightly lower than the Webster-Yang index (0.65). The index derived from the MME is generally better

than that derived from individual models. The spread among different realizations of individual models is generally smaller than that of the western North Pacific monsoon index (Figure 4), indicating a weaker internal variability. In observation, the year-to-year variation of the Australian monsoon is significantly dominated by El Nino or tropical Pacific forcing (Figure 7d). The responses of most models, 10 out of 13, are stronger than the reanalysis (Figure 7d). The strong tropical Pacific forcing suppresses the internal noise in the model response. Models having larger spread among different realizations (Figure 4d), i.e. GFDL and NCEP, usually have weaker responses to tropical Pacific forcing (Figure 7d).

The Australian monsoon shows a weak decreasing tendency in the past decades, with a rate of -0.19 per 49 yrs (Figure 5d), which is not statistically significant at the 5% level. Similar change is also evident in the monsoon precipitation (Zhou et al. 2008b). This weakening trend is reproduced in most models but with relatively higher rates. Spread is evident among different realizations of the ensemble simulation (Figure 6d), indicating the necessity of employing ensemble technique, although the external tropical Pacific forcing to the interannual variation of Australian monsoon is strong.

e) East Asian monsoon

The most prominent feature of the East Asian summer monsoon variability is the weakening trend in the past decades (Figure 1e). Associated with this weakening tendency, precipitation has increased over the middle and lower reaches of the

Yangtze River valley, whereas it has decreased in North China (Hu 1997; Hu et al. 2003; Yu et al. 2004; Yu and Zhou 2007). This marked summer precipitation change is often called “Southern flood and Northern drought” pattern. Inspection on Figure 1e shows an out of phase relationship between the MME and the reanalysis in describing the long-term change. This disappointing result is quantitatively confirmed by the negative correlation between the reanalysis and the MME shown in Figure 3. All individual models also show negative correlations with the reanalysis, except for NCEP model (which is however still not statistically significant at the 5% level). The poor correspondence between the reanalysis and the MME is also evident in Figure 5e. The reanalysis shows a weakening trend at a rate of -2.7 per 50years, which is statistically significant at the 5% level. However, all individual models show positive trends, with 10 of them are statistically significant at the 5% level, except for NCEP model which shows nearly no trend. The SLP-based East Asian monsoon index is weakly related to tropical Pacific forcing in the reanalysis (Figure 7e). The responses of C20C models are quite spread in this regard. The implication of the strong anti-correlation in Figure 3 will be discussed in the following Section 4.

Since the observed monsoon change is outside of the range of ensemble mean model responses (Figure 5e), we further compare the observations with ensemble members in Figure 6e. The observation is outside the range of the spread of available 106 ensemble members. Since the observed decadal change of East Asian monsoon SLP index is outside of the range of the ensemble mean and ensemble

spread, we conclude that the EASM is ***poorly modeled*** in the sense described in section 2.

It should be noted that the SLP index actually measures the East Asian monsoon in the context of zonal land-sea thermal contrast. Above results suggest that the past 50 years variation of the zonal thermal contrast is poorly modeled. This conclusion may not always apply to the meridional land-sea thermal contrast, as partly evidenced in the simulated Webster-Yang index presented above. We further examine the simulated variation of East Asian summer monsoon measured by the meridional wind (Figure 1f). The results of 10 models are available and compared. In reanalysis the decreasing tendency of East Asian summer monsoon also stands out in the index derived from meridional wind. The MME mean shows some resemblance with the reanalysis (Figure 1f), having a correlation coefficient of 0.46, which is statistically significant at the 5% level (Figure 3). Among the 10 models analyzed, the SOCOL and HadAM3 model have relatively high correlation coefficients, which are above 0.47 and statistically significant at the 1% level. For the ensemble mean of HadAM3, the skill of East Asian monsoon variation is comparable to the Australian monsoon and western North Pacific monsoon, and higher than that of Webster-Yang index and Indian monsoon (Figure 3). In the SOCOL model, the skill of East Asian monsoon variation measured in terms of meridional wind is better than the other indices, and comparable to the Webster-Yang index. The weakening tendency of the meridional wind is partly reproduced in the MME except with a weaker rate, with -1.85 per 50year in the

MME versus -2.76 per 50year in the reanalysis; both are statistically significant at the 5% level. Half of the 10 models fail in significantly reproducing this trend (Figure 5f). Some models such as SOCOL and HadAM3 are better than the MME. The spreads among different realizations are not large in these two models (Figure 6f). The MME is not always the best and this condition is similar to the Indian monsoon circulation.

The strength of meridional wind response to tropical Pacific forcing is generally weak and it is rarely captured by the models considered (Figure 7f). In addition, since the trend of observation is outside the range of the spread among 106 ensemble members (Figure 6f), there might be other supplementary mechanisms such as atmosphere-land interaction that could potentially modulate the East Asian monsoon variability (Liu and Yanai, 2002; Yang and Lau, 2006). These supplementary mechanisms are however not included in our simulations.

Based on the results of two East Asian summer monsoon indices, we conclude that the past variation of zonal land-sea thermal contrast is poorly modeled, while that of the meridional wind index is partly forced and reproducible, since four models show useful skills. Most models can not simulate the observed East Asian monsoon circulation variability; this does not necessarily indicate that the SST alone is not sufficient to reproduce the observed variability. It also could be due to the missing of important physical processes and incorrect parameterization of sub-grid scale processes in these climate models. The missing of ocean-atmosphere

interaction in these AMIP simulations may also play a role (Wang et al. 2005; Zhou et al. 2008a,c).

In addition, the East Asian summer monsoon index as defined by SLP difference between 110°E and 160°E should be rather similar to the meridional wind index based on the geo-strophic relation. Above analyses show that the models perform poorly in simulating the long-term trend of the SLP difference, but do relatively better (although still not good) in simulating the trend of meridional wind index. Why is the model performance so different for these two indices? A further examination found that while these two indices are highly correlated with each other in the reanalysis, having a correlation coefficient higher than 0.90, the correlations are low (less than 0.4) in most models. The relationships between the SLP and the meridional wind indices are sensitive to the mean states of individual models. Since climate models generally have biases in the mean states, a simple definition of the index as the observation may not be always accurate. In several models, the bias in the climate mean position of western Pacific subtropical high has led to a poor correlation between the indices derived from SLP and meridional wind (figures not shown). This may raise a new question for the evaluation of model performances over the East Asian domain.

4. Discussion on the forcing mechanism

Above analyses reveal how reproducible different components of the A-AM circulation system are. Regression analysis presented above (Figure 7) suggests that

most monsoon circulation variations come from the external SST forcing. To identify the possible forcing mechanism, we perform correlation analysis. Since both the South Asian monsoon measured by the Webster-Yang index and the Australian monsoon variation are better reproduced than the others, we begin our analysis from these two components. The simultaneous correlations of the observed and simulated Webster-Yang indices with the SST anomalies are shown in Figures 8a-b. In the observations, both the equatorial central-eastern Pacific and the tropical western Indian Ocean show significant negative correlations, displaying the role of remote El Nino forcing and the local SST effect (Figure 8a). It is not surprising to see that the MME closely resembles the observation (Figure 8b). The high reproducibility of South Asian monsoon circulation mainly comes from tropical Pacific forcing. This is consistent with many previous studies (See Yang and Lau 2006; Lau and Wang 2006 for comprehensive reviews). For the negative SSTA in the western Indian Ocean, we have calculated the lead/lag correlations and found the correlation between the monsoon and SSTs in the previous winter and spring is relatively low, which is far different from that in the eastern tropical Pacific (figures not shown here), hence it is more likely that a strong South Asian monsoon causes the stronger cross-equatorial wind, which further cools the western Indian Ocean. This relationship is different from that on the tropical biennial oscillation (TBO) time scale (e.g., Li et al. 2001). The difference of Indian Ocean SST and Asian monsoon relationship on TBO (1.5-3 yr) and ENSO (3-7 yr) time scales have been documented in previous studies (e.g., Chang and Li 2000; Li and Zhang 2002). Note

the South Asian monsoon in terms of Webster-yang index includes most parts of the A-AM components analyzed. It represents a measure of the strength of large-scale forcing.

The map of correlation coefficients of the Australian monsoon index with the SST anomalies is shown in Figure 8c for the observation. Significant negative correlations are evident in the equatorial central-eastern Pacific and the tropical Indian Ocean, along with positive correlations in the western Pacific, subtropical South and North Pacific. This pattern also indicates an El Nino-type forcing. The map for the MME is shown in Figure 8d, which closely resembles that of the observation except for the North Pacific sector. Hence most simulated variability of the Australian monsoon arises from tropical Pacific forcing.

For the variations of western North Pacific monsoon, a weaker forcing is seen in the equatorial central Pacific (Figure 8e). Significant negative correlations are evident in the western Pacific around the maritime continent, tropical eastern Indian Ocean, South China Sea, western North Pacific and South Pacific convergence zone (Figure 8e). The forcing in the MME is underestimated in the MC region but well reproduced in the tropical eastern Indian Ocean (Figure 8f). However, a weak signal in Figs.8e-f does not mean that the tropical Pacific has no impact on the western North Pacific monsoon. Previous studies demonstrated that the western North Pacific monsoon has a 6-months lagged response to El Nino forcing during the El Nino decaying summer when the SSTA is about normal in the eastern Pacific (Wang et al. 2000; Wang and Zhang 2002; Li and Wang 2005). In Figure 9 we plot

the lagged correlation of summer monsoon index with previous winter (DJF) SSTA. Significant negative correlations stand out in the central and eastern Pacific, confirming previous studies in that the western Pacific summer monsoon tends to weaken in the El Nino decaying summer. The MME resembles the observation in spatial pattern (cf. Figure 9a and Figure 9b). This significant negative correlation/regression is well captured by most models (Figure 9c).

The effect of SST on the Indian monsoon is divided into "remote effect" by the tropical central-eastern Pacific SST and "local effect" by the regional SSTs of tropical-extratropical oceans near the Asian continent (Li et al. 2005; Yang and Lau 2006), although the local effect from the Indian Ocean may be triggered by the tropical Pacific Ocean (e.g. Lau and Nath 2003; Cherchi et al. 2007). In the observations, the interannual variability of Indian monsoon is connected to El Nino, as evidenced by the moderate negative correlations in the equatorial eastern Pacific (Figure 10a, see also Figure 7b). In the ensemble simulation, however, significant negative (positive) correlations are evident in the equatorial central-eastern Pacific (western Pacific) (Figure 10b). This difference suggests that the tropical Pacific forcing should not be the unique mechanism dominating the Indian monsoon variability, as suggested by many previous studies (e.g., Chang et al. 2001; Liu and Yanai 2002). Note that we evaluate the result for the whole 1950-1999 period. There is an interdecadal change in monsoon-ENSO relationship (Wang et al. 2008). The Indian monsoon-ENSO connection has weakened in recent decades (Kumar et al. 1999) and the division of the 1950-1999 period into two subsets before and after

1976 would provide stronger connection in the former (Kinter et al. 2002; Cherchi and Navarra 2007). For example, the correlation between the MME and the reanalysis is 0.38 (0.26) for the period of 1950-1976 (1976-1999).

The forcing mechanism of East Asian summer monsoon is more complex. In the observations, the western Pacific and tropical Indian Ocean are cold, while the North Pacific is warm (Figure 10c). The pattern of SST anomalies in the MME is, however, nearly out of phase with that of the observations (cf. Figure 10c and Figure 10d). This is consistent with Figure 3, which shows significant negative correlations between the simulated and observed monsoon indices. The decadal change of East Asian summer monsoon concurred with the 1976-1977 climate shift, which was associated with SST fluctuations in the tropical Indian Ocean and Pacific Oceans (Deser et al. 2004). While the tropical Indian Ocean had a warming trend in the past decades, the midlatitude North Pacific exhibited a cooling change (Trenberth et al. 2007). In our model results, the forcing of tropical Indian Ocean warming and North Pacific cooling has produced an intensified (rather than weakened) zonal land-sea thermal contrast over the East Asian monsoon domain.

Whether or not the ocean SST forcing contributes to the East Asian monsoon variation remains an open question, because the weak response of AGCMs to the prescribed SST forcing outside of the tropics might also explain the failure of C20C models in this regard (Kushnir et al. 2002). Additional study is needed to understand the physical processes behind this failure, including the sensitivity of model response to its horizontal resolutions. Recent observational analysis found that the

weakening tendency of East Asian summer monsoon is partly dominated by a cooling trend over the middle troposphere of East Asia (Yu et al. 2004; Yu and Zhou 2007). This troposphere cooling trend can not be reproduced by specifying SST in the experiments (figures not shown here). In addition, the strong anti-correlation in Figure 3 and Figure 10d indicates a strong but spurious relationship of the monsoon with SST in these simulations. There is a possibility that the SST change was at least partly forced by changes in the East Asian summer monsoon rather than vice versa, as proposed previously by Wang et al. (2005). The difficulty of simulating East Asian summer monsoon variation with specified SST was also discussed by Zhou et al. (2008c).

The map of correlation coefficients of the East Asian monsoon meridional wind index with SST anomalies is shown in Figure 10e. The SST anomaly pattern is similar to that of Figure 10c as expected. The simulation partly resembles the observation in negative correlations over the tropical Indian Ocean (Figure 10f), suggesting the observed Indian Ocean warming has weakened the meridional land-sea thermal contrast and partly explains the observed weakening tendency of the East Asian summer monsoon. Thus, the strategy of specifying ocean surface conditions such as SST fails in capturing zonal land-sea thermal contrast change, but partly succeeds in capturing meridional wind variation. Most signals here come from the tropical Indian Ocean and western North Pacific forcing. How does the Indian Ocean SSTA play a role in impacting the long-term change of East Asian summer monsoon? In addition to its direct impact on the meridional land-sea

thermal contrast, Zhou et al. (2008d) suggested that a warming Indian Ocean - western Pacific are in favor of the westward extension of the western Pacific subtropical high via the negative heating in the central and eastern tropical Pacific and increased monsoon condensational heating in the equatorial Indian Ocean/maritime continent.

Finally, comparisons of the observations with the MME in Figures 8 -10 only provide a reference for the identification of possible forcing mechanisms. Assuming the observation as one member, the correlation of an ensemble mean with the SST does not contain as much internal variability as the observations, we may not say that the models have higher or lower correlations with SST than the observations. To make the simulation and the observations comparable, we calculate the correlation of SST anomalies with the monsoon index derived from each realization, and then measure its resemblance with that of the observation by calculating pattern correlation coefficient. To measure the resemblance of each realization with the MME, similar calculation is done between the MME and each realization. The pattern correlations of SST anomalies for each realization with that for the reanalysis and the MME mean is shown in Figure 11. There are spreads among the total 106 realizations, indicating the SST anomalies associated with the MME may not always represent that associated with individual realizations. However, most individual realizations merge towards the MME, suggesting it is informative to analyze the results of MME. The linear relationships in Figure 11 indicate that for each individual realization a better resemblance to the MME generally follows a better resemblance to the observation.

Hence it is reasonable to compare the observed and the MME simulated monsoon correlations with the SST. It is interesting to note that the result of East Asian monsoon SLP index is quite noisy even within different realizations of a same model, indicating a low reproducibility with prescribed SST forcing. The situation of Indian monsoon index is a bit better, however, still not as good as the other monsoon indices. This scatter plot can serve as a useful tool for measuring and comparing the reproducibility of different monsoon indices.

In addition, we have also examined the indices for June to September (JJAS) average, the order of reproducibility for different monsoon circulations keeps unchanged (figures not shown), although the skills for JJAS are slightly higher than that for JJA due to the intensified SST signals in the tropical eastern Pacific associated with ENSO in September (cf. Figure 3b of Wang et al. 2008). For example, the correlation coefficient between the observed and the MME simulated Indian monsoon circulation indices has increased from 0.32 of JJA to 0.39 of JJAS. This result is consistent with Kucharski et al. (2008), who found that the JJAS averaged pan-Indian monsoon area precipitation has a better reproducibility than that of JJA.

5. Summary

An attempt has been made in the present study to identify and understand which components of the Asian-Australian monsoon circulation variations are forced and reproducible. This effort has been facilitated by the availability of

ensemble experiments of about 13 AGCMs involved in the CLIVAR C20C project. The large sample size generated in the C20C coordinated experiments encourages the implementation of multi-model ensemble, which is a useful way for removing disturbance of model-dependent internal noise. The priority of different components of the A-AM circulations in terms of reproducibility is assessed by comparing the simulated and observed late 20th century (1950-1999) monsoon circulation variation. These results should be helpful to the physical understanding on the 20th century evolution of the A-AM system. The main findings are listed below.

1) Among the subsystems of the A-AM, the South Asian and the Australian monsoon circulations are forced and well modeled, as evidenced in their high reproducibility. The western North Pacific monsoon circulation is also forced and well modeled except with a slightly lower reproducibility.

2) The remote equatorial central-eastern Pacific SSTs forcing is the primary forcing mechanism for the observed variability of the South Asian and the Australian monsoon circulations. The western North Pacific monsoon circulation has a lagged response to El Nino forcing during the El Nino decaying summer when the SSTA is about normal in the eastern Pacific. The simultaneous SST forcing comes from the western Pacific surrounding the marinetime continent.

3) The Indian monsoon circulation has a moderate reproducibility. In observation, the JJA Indian monsoon circulation shows relatively weak correlations with simultaneous SST in the tropical eastern Pacific during 1950-1999, mainly due to the weakened Indian monsoon-ENSO connection in recent decades.

4) Among the A-AM subsystems, the East Asian summer monsoon has the lowest reproducibility and is poorly modelled, especially in terms of the zonal land-sea thermal contrast. None of the models used here reproduces the observed weakening tendency of the zonal land-sea thermal contrast across East Asia through either SST-forced or internal variability or a combination of both. However, the tropical Indian Ocean SST forcing partly reproduces the meridional wind variation over East Asia in several models.

5) For the Webster-Yang index, the Western North Pacific monsoon index, and the Australian monsoon index, the indices derived from the MME is always the best or at least comparable to that of the best model. For the Indian monsoon and the East Asian monsoon indices, however, the MME may not always be the best, the results of some models are better than the MME.

Acknowledgments:

This work contributes to CLIVAR C20C project and is jointly supported by the Major State Basic Research Development Program of China (973 Program) under grant No. 2006CB403603, 2005CB321703 and the National Natural Science Foundation of China under grant Nos. 40523001, 40625014 and 40221503. Adam Scaife and Chris Folland were supported by the "Defra and MoD Integrated Climate Programme-GA01101, CBC/2B/0417_Annes C5". P. Sporyshev was supported by the Russian Foundation for Basic Research.

References

Chang CP, Harr P, Ju J (2001) Possible Roles of Atlantic Circulations on the Weakening Indian Monsoon Rainfall–ENSO Relationship. *J Clim* **14**: 2376-2380

Chang CP, Zhang Y, Li T (2000a) Interannual and interdecadal variations of the East Asian summer monsoon and tropical Pacific SSTs. Part I: Role of the subtropical ridge. *J Clim* **13**: 4310-4325

Chang CP, Zhang Y, Li T (2000b) Interannual and interdecadal variations of the East Asian summer monsoon and tropical Pacific SSTs. Part II: Meridional structure of the monsoon. *J Clim* **13**: 4310-4325

Chang CP, Li T (2000) A theory of the tropical tropospheric biennial oscillation. *J. Atmos. Sci.*, **57**, 2209-2224.

Cherchi A, Navarra A (2003) Reproducibility and predictability of the Asian summer monsoon in the Echam4 GCM. *Clim Dyn* **20**: 365-379

Cherchi A, Navarra A (2007) Sensitivity of the Asian summer monsoon to the horizontal resolution: differences between AMIP-type and coupled model experiments. *Clim Dyn* **28**: 273-290

Cherchi A, Gualdi S, Behera S, Luo JJ, Masson S, Yamagata T, Navarra A (2007) The influence of tropical Indian Ocean SST on the Indian summer monsoon. *J Clim* **20**: 3083-3105

Collins WD, et al. (2003) Description of the NCAR Community Atmosphere Model (CAM2). National Center for Atmospheric Research, Boulder, Colo., USA

Deser C, Phillips AS, Hurrell JW (2004) Pacific interdecadal climate variability: Linkages between the tropics and the north Pacific during boreal winter since 1900. *J Clim* **17**: 3109-3124

Fennessy MJ, Kinter JL, Kirtman B, Marx L, Nigam S, Schneider E, Shukla J, Straus D, Vernekar A, Xue Y, Zhou J (1994) The simulated Indian monsoon: A GCM senstivity study. *J Clim* **7**: 33-43

Folland CK, Shukla J, Kinter J, Rodwell MJ (2002) C20C: The Climate of the Twentieth Century Project. CLIVAR Exchanges, Vol 7, No2 (June 2002) 37-39. http://www.clivar.org/publications/exchanges/ex24/ex24.pdf

Gadgil S, Sajani S (1998) Monsoon precipitation in the AMIP runs. *Clim Dyn* **14**: 659-689

Guo QY (1983) The summer monsoon intensity index in East Asia and its variation. *Acta Geogr Sinica* **38:** 207-217 (in Chinese)

Gong DY, and Ho CH (2002), Shift in the summer rainfall over the Yangtze River valley in the late 1970s. *Geophys. Res. Lett.*, **29**, 1436, doi:10.1029 /2001GL014523.

Hu ZZ (1997) Interdecadal variability of summer climate over East Asia and its association with 500 hPa height and global sea surface temperature. *J Geophys Res* **102**: 19403–19412

Hu ZZ, Yang S, Wu R (2003) Long-term climate variations in China and global warming signals. *J Geophys Res.* doi:10.1029/2003JD003651

Ju J, Slingo J (1995) The Asian summer monsoon and ENSO. *Q J R Meteorol Soc* **121**:

1133-1168

Kalnay, E., and Coauthors (1996) The NCEP/NCAR 40-year Reanalysis Project, *Bull. Am. Meteorol. Soc*, **77**, 437-471.

Kang IS, Jin K, Lau KM, Shukla J, et al. (2002) Intercomparison of Atmospheric GCM simulated anomalies associated with the 1997/98 El Nino. *J Clim* **15**: 2791-2805

Kang IS, Shukla J (2006) Dynamic seasonal prediction and predictability of the monsoon. In: Wang B (ed) The Asian Monsoon. Springer/Praxis Publishing, New York, pp 585-612

Kinter III JL, Miyakoda K, Yang S (2002) Recent changes in the connection from the Asian monsoon to ENSO. *J Clim* **15**: 1203-1215

Krishnamurti TN, Vijaya Kumar TSV, Mitra AK (2006) Seasonal climate prediction of Indian summer monsoon. In: Wang B (ed) The Asian Monsoon. Springer/Praxis Publishing, New York, pp 553-583

Kumar KK., Rajagopalan B, Kane MA (1999) On the weakening relationship between the Indian monsoon and ENSO. *Science* **284**: 2156-2159

Kushnir Y, Robinson WA, Blade I, et al. (2002) Atmospheric GCM Response to Extratropical SST Anomalies: Synthesis and Evaluation. *J Clim* **15**: 2233-2256

Kucharski F, Scaife AA, Yoo JH, Folland CK, et al. (2008) The CLIVAR C20C Project. Skill of simulating Indian monsoon rainfall on interannual to decadal timescale: Does GHG forcing play a role? *Clim Dyn*, DOI 10.1007/s00382 -008-0462-y

Lau NC, Nath MJ (2000) Impact of ENSO on the variability of the Asian-Australian monsoons as simulated in GCM experiments. *J Clim* **13**: 4287-4309

Lau N.-C., Nath M. J. (2003) Atmosphere-Ocean variations in the Indo-Pacific sector during ENSO episodes. *J Clim* **16**: 3-20

Lau N.-C., Wang B (2006) Interactions between the Asian monsoon and the El Nino/Southern Oscillation. In: Wang B (ed) The Asian Monsoon. Springer/Praxis Publishing, New York, pp 479-512

Li T, Wang B (2005) A review on the western North Pacific monsoon: synoptic-to-interannual vriabilities. *Terrestrial, Atmospheric and Oceanic Science*s, **16**, 285-314.

Li T, Zhang Y (2002) Processes that determine the quasi-biennial and lower-frequency variability of the South Asian monsoon. *J. Meteor. Soc. Japan*, **80**, 1149-1163.

Li T, Zhang YC, Chang CP, Wang B (2001) On the relationship between Indian Ocean SST and Asian summer monsoon. *Geophy. Res. Let.*, **28**, 2843-2846.

Li T, Tung YC, Hwu JW (2005) Remote and local SST forcing in shaping Asian-Australian monsoon anomalies. *J Meteorol Soc Japan* **83**: 153-167

Li T, Liu P, Fu X, Wang B (2006) Spatiotemporal structures and mechanisms of the tropospheric biennial oscillation in the Indo-Pacific warm ocean regions. *J Clim* **19**: 3070-3087

Liu X, Yanai M (2002) Influence of Eurasian spring snow cover on Asian summer rainfall. *Int J Climatol* **22**: 1175-1089

McBride JL (1987) The Australian summer monsoon. In: Chang CP, Krishnamurti TN (ed) Monsoon Meteorology. Oxford University Press, pp 203-231

Parthasarathy B, Rupakumar K, Munot AA (1991) Evidence of secular variations in Indian monsoon rainfall-circulation relationships. *J Clim* **4**: 927-938

Rayner NA, Parker DE, Horton EB, Folland CK, Alexander LV, Rowell DP, Kent EC, Kaplan A (2003) Global analyses of SST, sea ice and night marine air temperature since the late nineteenth century. *J Geophys Res.* doi:10.1029/2002JD002670

Scaife AA, Kucharski F, Folland CK, Kinter J, et al. (2008) The CLIVAR C20C Project: Selected 20th century climate events. *Clim Dyn*, DOI 10.1007/s00382-008-0451-1

Sperber KR, Palmer TN (1996) Interannual Tropical rainfall variability in general circulation model simulations associated with the Atmospheric Model Intercomparison Project. *J Clim* **9**: 2727-2750

Sperber KR, Brankovic C, Deque M, Frederiksen CS, Graham, R., and co-authors (2001) Dynamical seasonal predictability of the Asian summer monsoon. *Mon Wea Rev* **129**: 2226-2248

Trenberth KE, Jones PD, Ambenje P, Bojariu R, Easterling D, Klein Tank A, Parker D, Rahimzadeh F, Renwick JA, Rusticucci M, Soden B, Zhai P (2007) Observations: Surface and Atmospheric Climate Change. In: Solomon S, Qin D, Manning M, Chen Z, Marquis M, Averyt KB, Tignor M, Miller HL (ed) Climate Change 2007: The Physical Science Basis. Contribution of Working Group I to the Fourth Assessment Report of the Intergovernmental Panel on Climate

Change. Cambridge University Press, Cambridge, United Kingdom and New York, NY, USA

Turner AG, Inness PM, Slingo JM (2005) The role of the basic state in the ENSO-monsoon relationship and implications for predictability. *Q J R Meteorol Soc* **131**: 781-804

Uppala SM, Kallberg PW, Simmons AJ, et al. et al. (2005) The ERA-40 re-analysis. *Q J R Meteorol Soc* **131**: 2961-3012

Wang H (2001) The weakening of Asian monsoon circulation after the end of 1970's. *Adv Atmos Sci* **18**: 376-386

Wang B, Wu R, Fu X (2000) Pacific-East Asia teleconnection: How does ENSO affect East Asian climate? *J Clim* **13**:1517-1536

Wang B, Wu R, Lau KM (2001) Interannual Variability of the Asian Summer Monsoon: contrasts between the Indian and the Western North Pacific-East Asian Monsoons. *J Clim* **14**: 4073-4090

Wang B, Zhang Q (2002) Pacific-East Asian teleconnection, part Ⅱ: How the Philippine Sea anticyclone established during development of El Nino. *J Clim* **15**:3252-3265

Wang B, Kang IS, Lee JY (2004) Ensemble Simulations of Asian–Australian Monsoon Variability by 11 AGCMs. *J Clim* **17**: 803-818

Wang B, Ding QH, Fu XH, Kang IS, Jin K, Shukla J, Doblas-Reyes F (2005) Fundamental challenge in simulation and prediction of summer monsoon rainfall. *Geophys Res Lett.* doi:10.1029/2005GL022734

Wang B, Ding Q (2006) Changes in global monsoon precipitation over the past 56 years. *Geophys Res Lett.* doi:10.1029/2005GL025347

Wang B (2006) The Asian Monsoon. Springer/Praxis Publishing, New York.

Wang B, Yang J, Zhou T, Wang B (2008) Interdecadal changes in the major modes of Asian–Australian monsoon variability: Strengthening relationship with ENSO since the late 1970s. *J Clim* **21**: 1771-1789

Webster PJ, Yang S (1992) Monsoon and ENSO: Selectively interactive systems. *Q J R Meteorol Soc* **118**: 877-926

Wu R, Kirtman BP (2005) Roles of Indian and Pacific Ocean air-sea coupling in tropical atmospheric variability. *Clim Dyn* **25**: 155-170

Wu R, Kirtman B, Pegion K (2006) Local air-sea relationship in observations and model simulations. *J Clim* **19:** 4914-4932

Yang S, Lau KM (2006) Interannual variability of the Asian monsoon. In: Wang B (ed) The Asian Monsoon. Springer/Praxis Publishing, New York, pp 259-293

Yu R, Wang B, Zhou T (2004) Tropospheric cooling and summer monsoon weakening trend over East Asia. *Geophys Res Lett.* doi:10.1029 /2004GL021270

Yu R, Zhou T (2007) Seasonality and three-dimensional structure of the interdecadal change in East Asian monsoon. *J Clim* **20**: 5344-5355

Zhou T, Li Z (2002) Simulation of the East Asian summer monsoon by using a variable resolution atmospheric GCM. *Clim Dyn* **19**: 167-180

Zhou T, Yu R (2005) Atmospheric water vapor transport associated with typical anomalous summer rainfall patterns in China. *J. Geophys. Res.* doi:10.1029/

2004JD005413.

Zhou T, Yu R (2006) Twentieth century surface air temperature over China and the globe simulated by coupled climate models. *J Clim* 19: 5843-5858

Zhou T, Wu B, Wang B (2008a) How well do Atmospheric General Circulation Models capture the leading modes of the interannual variability of Asian-Australian Monsoon? *J Clim*, in Press

Zhou T, Zhang L, Li H (2008b) Changes in global land monsoon area and total rainfall accumulation over the last half century, *Geophys. Res. Lett.*, **35**, L16707, doi:10.1029/2008GL034881.

Zhou T, Yu R, Li H, Wang B (2008c) Ocean forcing to changes in global monsoon precipitation over the recent half century. *J Clim*, **21:** 3833–3852.

Zhou T, Yu R, Zhang J, Drange H, Cassou C, Deser C, Hodson D L R, Sanchez-Gomez E, Li J, Keenlyside N, Xin X, Okumura Y (2008d), Why the Western Pacific Subtropical High has Extended Westward since the Late 1970s. *J. Clim*, In revision

Zhu C, Lee WS, Kang H, Park CK (2005) A proper monsoon index for seasonal and interannual variations of the East Asian monsoon. *Geophys Res Lett.* doi:10.1029/2004GL021295

Table 1 Description of models from C20C partners

No.	Research Centre	Model	Ensemble size	Remarks
1	NOAA/Geophysical Fluid Dynamics, USA	GFDL	10	SST, GHG, aerosols, ozone, solar, land cover, black carbon, volcano
2	Centre National de Recherches Meteorologiques, France	ARPEGE	1	SST, GHG, sulfate, aerosol, ozone
3	Centre for Ocean Land Atmosphere studies, USA	NCEP	4	Pacemaker experiment, prescribed SST in 165°-290°E,10°S-10°N
4	International Centre for Theoretical Physics, Italy	ICTP	10	SST
5	NASA Goddard Global Modeling and Assimilation Office, USA	NSIPP	14	SST
6	NCAR, USA	CAM2 (version 2.0.1)	12	SST
7	LASG/IAP, Chinese Academy of Sciences	GAMIL	4	SST, GHG, solar, sulfate aerosol
8	Met Office Hadley Centre for Climate Change, UK	HadAM3	11	SST, GHG, aerosols, ozone, solar, land cover
9	Institute for Atmospheric and Climate Science, ETH, Switzerland	SOCOL	9	SST, GHG, volcano, solar, land cover, coupled ozone
10	Centro Euro-Mediterraneo per i Cambiamenti Climatici (CMCC/INGV), Bologna, Italy	CMCC (Echam4.6)	6	SST, GHG, sulfate aerosols, ozone
11	Meteorological Research Institute, Japan	MRI	6	SST, CO2
12	Voeikov Main Geophysical Observatory, Russia	MGO	10	SST, GHG, volcano, solar
13	University of Maryland at College Park, USA	CABO	9	SST, volcano, solar, aerosol

Figure Captions

Figure 1 Time series of ensemble mean model simulations of: (a) Webster-Yang index, (b) Indian monsoon index, (c) Western North Pacific monsoon index, (d) Australian monsoon index, (e) East Asian summer monsoon index defined as zonal SLP difference, (f) East Asian monsoon index defined as meridional wind averaged over (20-45°N, 110-120°E). The time series were normalized and thus unit-less.

Figure 2 Standard deviations of different monsoon index time series. The abscissa numbers correspond to different monsoon indices. 1-Webster-Yang index, 2- Indian Monsoon index, 3-Western North Pacific monsoon index, 4- Australian monsoon index, 5-East Asian monsoon SLP difference index, 6-East Asian monsoon meridional wind index. Units are m/s for indices 1-4 and 6, and hPa for index 5.

Figure 3 Correlation coefficients between the monsoon indices derived from the ensemble simulation and the observation. The horizontal dashed line indicates the threshold of the correlation coefficient statistically significant at the 5% level. The abscissa numbers correspond to different monsoon indices. 1-Webster-Yang index, 2- Indian Monsoon index, 3-Western North Pacific monsoon index, 4- Australian monsoon index, 5-East Asian monsoon SLP difference index, 6-East Asian monsoon meridional wind index.

Figure 4 Correlation coefficients between the monsoon indices derived from different realizations of ensemble simulation and the observation. The correlations statistically significant at the 5% level are shown as red dots. The abscissa numbers correspond to different models. 1-GFDL, 2-ARPEGE, 3-NCEP, 4- ICTP, 5-NSIPP, 6-CAM2, 7-GAMIL, 8-HadAM3, 9-SOCOL, 10-CMCC, 11-MRI, 12-MGO, 13-CABO

Figure 5 Trends from 1950 to 1999 in the observation and ensemble means for the normalized (a) Webster-Yang index, (b) Indian monsoon index, (c) Western North Pacific monsoon index, (d) Australian monsoon index, (e) East Asian summer monsoon SLP index, (f) East Asian monsoon meridional wind index. Units are

"1/50yrs" except for the Australian monsoon the unit is 1/49yrs. The trends statistically significant at the 5% level are shown as red dots. The abscissa numbers correspond to the observation and different models. O-Observation, M-MME, 1-GFDL, 2-ARPEGE, 3-NCEP, 4-ICTP, 5-NSIPP, 6-CAM2, 7-GAMIL, 8-HadAM3, 9-SOCOL, 10-CMCC, 11-MRI, 12-MGO, 13-CABO.

Figure 6 Trends from 1950 to 1999 in the observation and different realizations for the normalized (a)Webster-Yang index, (b) Indian monsoon index, (c) Western North Pacific monsoon index, (d) Australian monsoon index, (e) East Asian summer monsoon SLP index, (f) East Asian monsoon meridional wind index. Units are "1/50yrs" except for the Australian monsoon the unit is 1/49yrs. The trends statistically significant at the 5% level are shown as red dots. The abscissa numbers correspond to the observation and different models: O-Observation, 1-GFDL, 2-ARPEGE, 3-NCEP, 4-ICTP, 5-NSIPP, 6-CAM2, 7-GAMIL, 8-HadAM3, 9-SOCOL, 10-CMCC, 11-MRI, 12-MGO, 13-CABO.

Figure 7 Strength of atmospheric response to tropical Pacific SST forcing. Regression coefficients between different normalized monsoon indices and simultaneous Nino 3 SST index are plotted. The regression coefficients statistically significant at the 5% level are shown as red dots. The abscissa numbers correspond to the observation and different models: O-Observation, M-MME, 1-GFDL, 2-ARPEGE, 3-NCEP, 4-ICTP, 5-NSIPP, 6-CAM2, 7-GAMIL, 8-HadAM3, 9-SOCOL, 10-CMCC, 11-MRI, 12-MGO, 13-CABO.

Figure 8 Spatial distributions of correlation coefficients between SSTs and Webster-Yang index (1st row), Australian monsoon index (2nd row), and western North Pacific monsoon index (3rd row) derived from the re-analysis (left column), and multi-model ensemble mean (right column). Only the correlations statistically significant at the 5% level are plotted.

Figure 9 Spatial distributions of correlation coefficients between previous winter (DJF) SSTs and western North Pacific summer monsoon index derived from (a) the

re-analysis, and (b) multi-model ensemble mean. Only the correlations statistically significant at the 5% level are plotted. (c) Regression coefficients between normalized western North Pacific summer monsoon index and previous winter Nino 3 SST index (Unit 1/k). The regression coefficients statistically significant at the 5% level are shown as red dots. The correspondence of abscissa numbers with the model names are the same as Figure 7.

Figure 10 Same as **Figure 8** except for the Indian monsoon (1st row), East Asian monsoon SLP index (2nd row), and the East Asian monsoon meridional wind index (3rd row). Only the correlations statistically significant at the 5% level are plotted.

Figure 11 Pattern correlation coefficient of SST anomalies associated with observed and modeled monsoon indices. The abscissa (ordinate) represents pattern correlation coefficients of SST anomalies between the observation (MME) and each individual simulation. Each dot represents one realization. (a) Webster-Yang index, (b) Indian monsoon index, (c) Western North Pacific monsoon index, (d) Australian monsoon index (e) East Asian monsoon SLP index (f) East Asian monsoon meridional wind index

Figure 1 Time series of ensemble mean model simulations of: (a) Webster-Yang index, (b) Indian monsoon index, (c) Western North Pacific monsoon index, (d) Australian monsoon index, (e) East Asian summer monsoon index defined as zonal SLP difference, (f) East Asian monsoon index defined as meridional wind averaged over (20-45°N, 110-120°E). The time series are normalized and thus unitless.

Figure 2 Standard deviations of different monsoon index time series. The abscissa numbers correspond to different monsoon indices: 1-Webster-Yang index, 2- Indian Monsoon index, 3-Western North Pacific monsoon index, 4-Australian monsoon index, 5-East Asian monsoon SLP difference index, 6-East Asian monsoon meridional wind index. Units are m/s for indices 1-4 and 6, and hPa for index 5.

Figure 3 Correlation coefficients between the monsoon indices derived from the ensemble simulation and the observation. The horizontal dashed line indicates the threshold of the correlation coefficient statistically significant at the 5% level. The abscissa numbers correspond to different monsoon indices: 1-Webster-Yang index, 2- Indian Monsoon index, 3-Western North Pacific monsoon index, 4-Australian monsoon index, 5-East Asian monsoon SLP difference index, 6-East Asian monsoon meridional wind index.

Figure 4 Correlation coefficients between the monsoon indices derived from different realizations of ensemble simulation and the reanalysis. The correlations statistically significant at the 5% level are shown as red dots. The abscissa numbers correspond to different models. 1-GFDL, 2-ARPEGE, 3-NCEP, 4- ICTP, 5-NSIPP, 6-CAM2, 7-GAMIL, 8-HadAM3, 9-SOCOL, 10-CMCC, 11-MRI, 12-MGO, 13-CABO

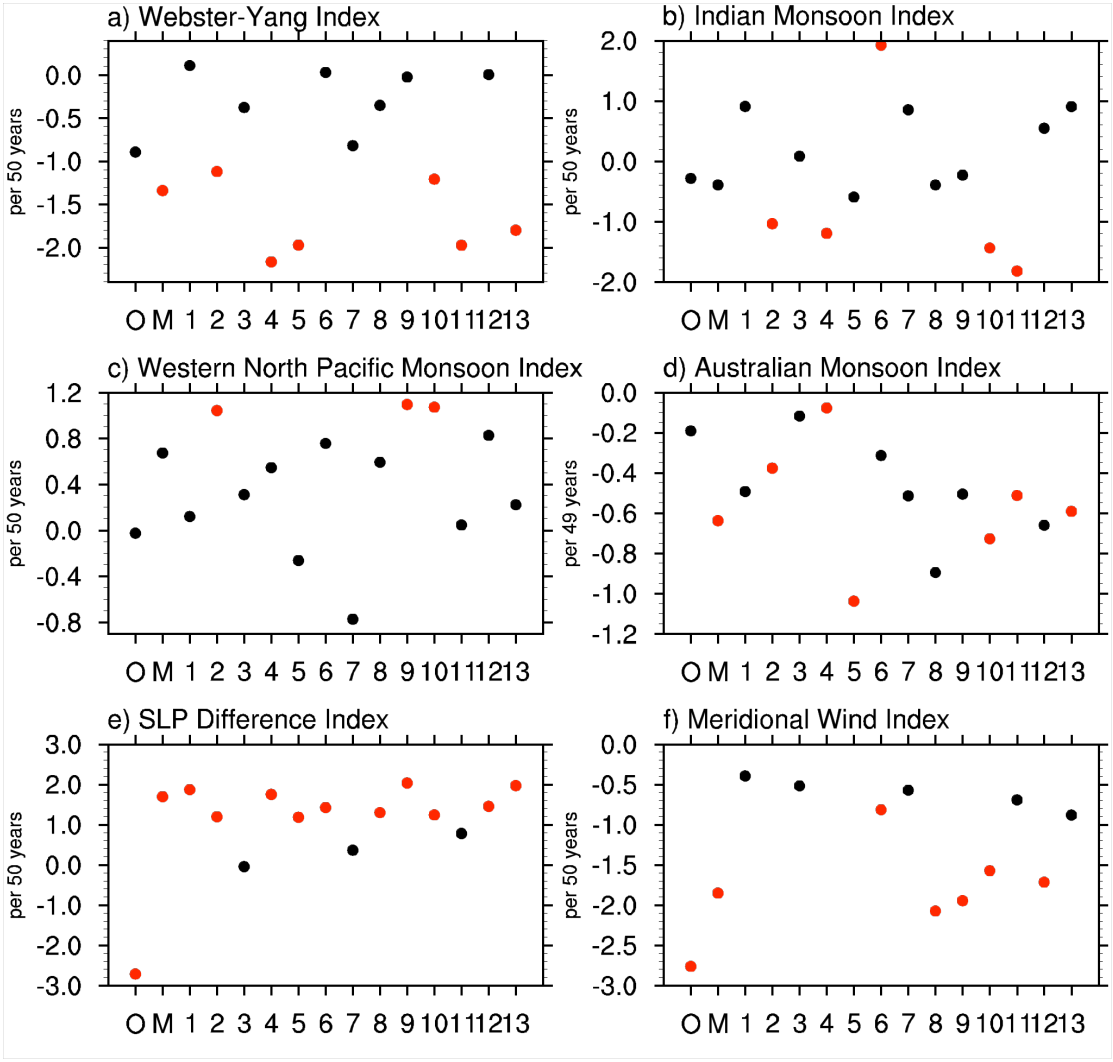

Figure 5 Trends from 1950 to 1999 in the observation and ensemble means for the normalized (a) Webster-Yang index, (b) Indian monsoon index, (c) Western North Pacific monsoon index, (d) Australian monsoon index, (e) East Asian summer monsoon SLP index, (f) East Asian monsoon meridional wind index. Units are "1/50yrs" except for the Australian monsoon the unit is 1/49yrs. The trends statistically significant at the 5% level are shown as red dots. The abscissa numbers correspond to the observation and different models. O-Observation, M-MME, 1-GFDL, 2-ARPEGE, 3-NCEP, 4-ICTP, 5-NSIPP, 6-CAM2, 7-GAMIL, 8-HadAM3, 9-SOCOL, 10-CMCC, 11-MRI, 12-MGO, 13-CABO.

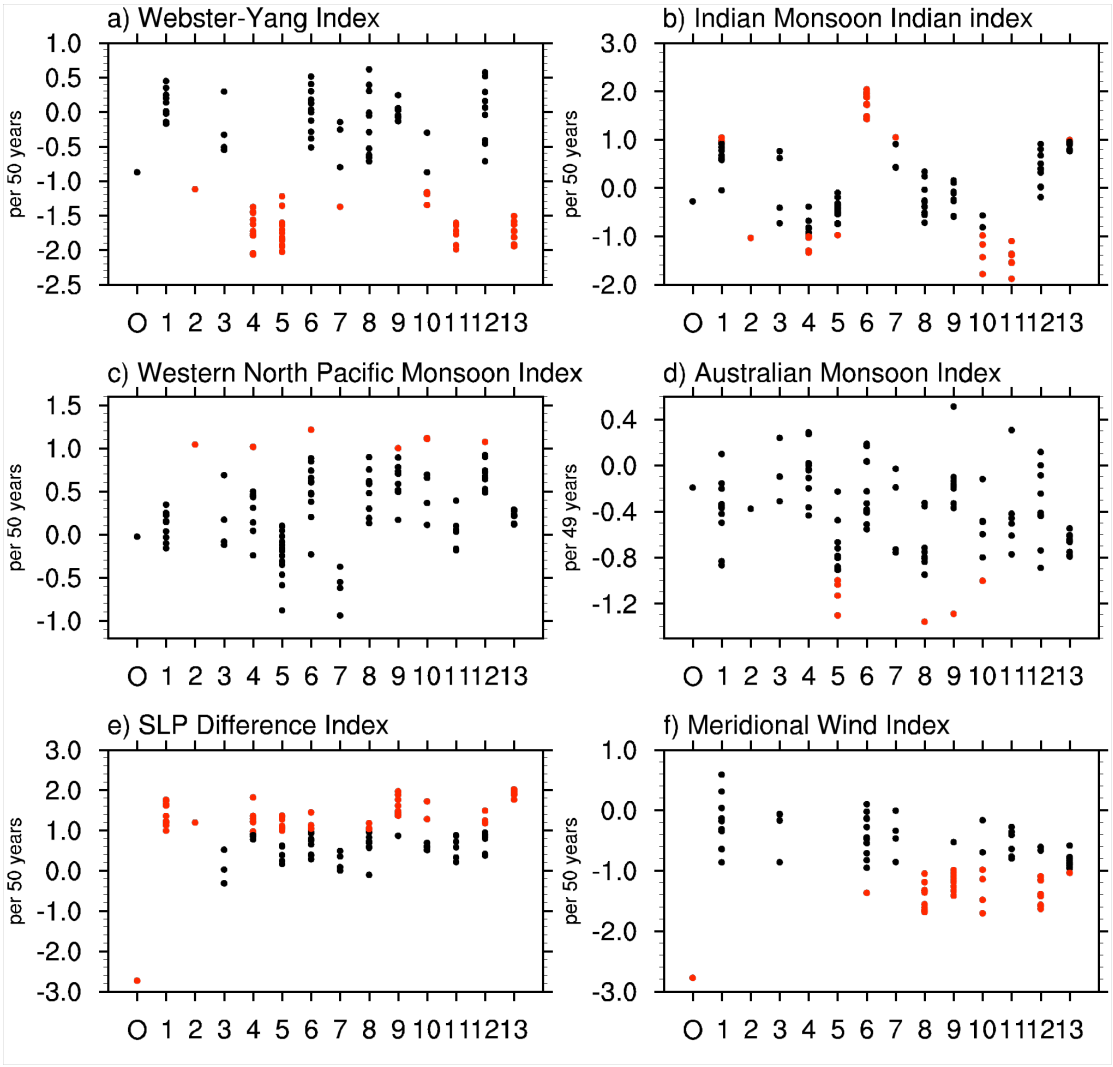

Figure 6 Trends from 1950 to 1999 in the observation and different realizations for the normalized (a)Webster-Yang index, (b) Indian monsoon index, (c) Western North Pacific monsoon index, (d) Australian monsoon index, (e) East Asian summer monsoon SLP index, (f) East Asian monsoon meridional wind index. Units are "1/50yrs" except for the Australian monsoon the unit is 1/49yrs.The trends statistically significant at the 5% level are shown as red dots. The abscissa numbers correspond to the observation and different models: O-Observation, 1-GFDL, 2-ARPEGE, 3-NCEP, 4-ICTP, 5-NSIPP, 6-CAM2, 7-GAMIL, 8-HadAM3, 9-SOCOL, 10-CMCC, 11-MRI, 12-MGO, 13-CABO.

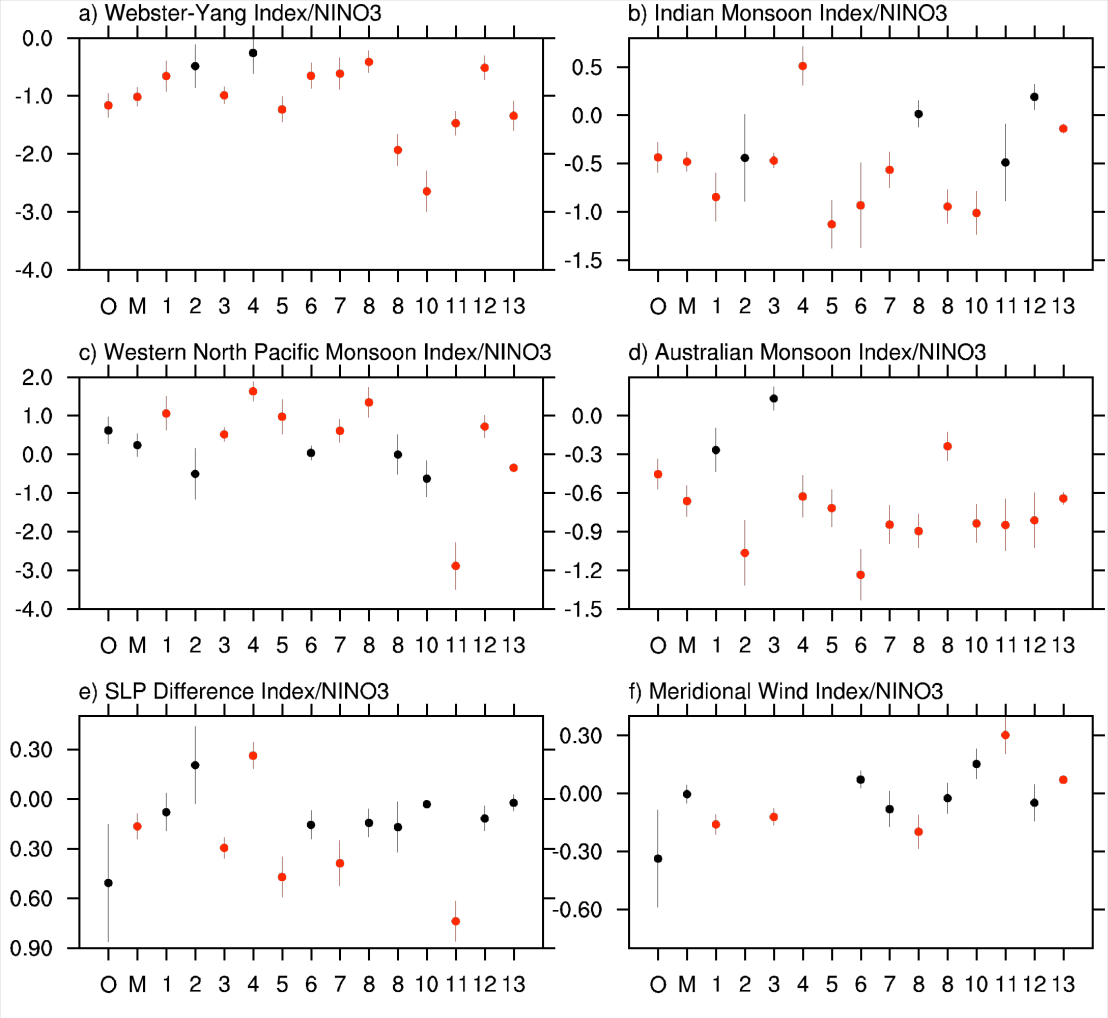

Figure 7 Strength of atmospheric response to tropical Pacific SST forcing. Regression coefficients between different normalized monsoon indices and simultaneous Nino 3 SST index are plotted. Units are "1/k". The regression coefficients statistically significant at the 5% level are shown as red dots. The abscissa numbers correspond to the observation and different models: O-Observation, M-MME, 1-GFDL, 2-ARPEGE, 3-NCEP, 4-ICTP, 5-NSIPP, 6-CAM2, 7-GAMIL, 8-HadAM3, 9-SOCOL, 10-CMCC, 11-MRI, 12-MGO, 13-CABO.

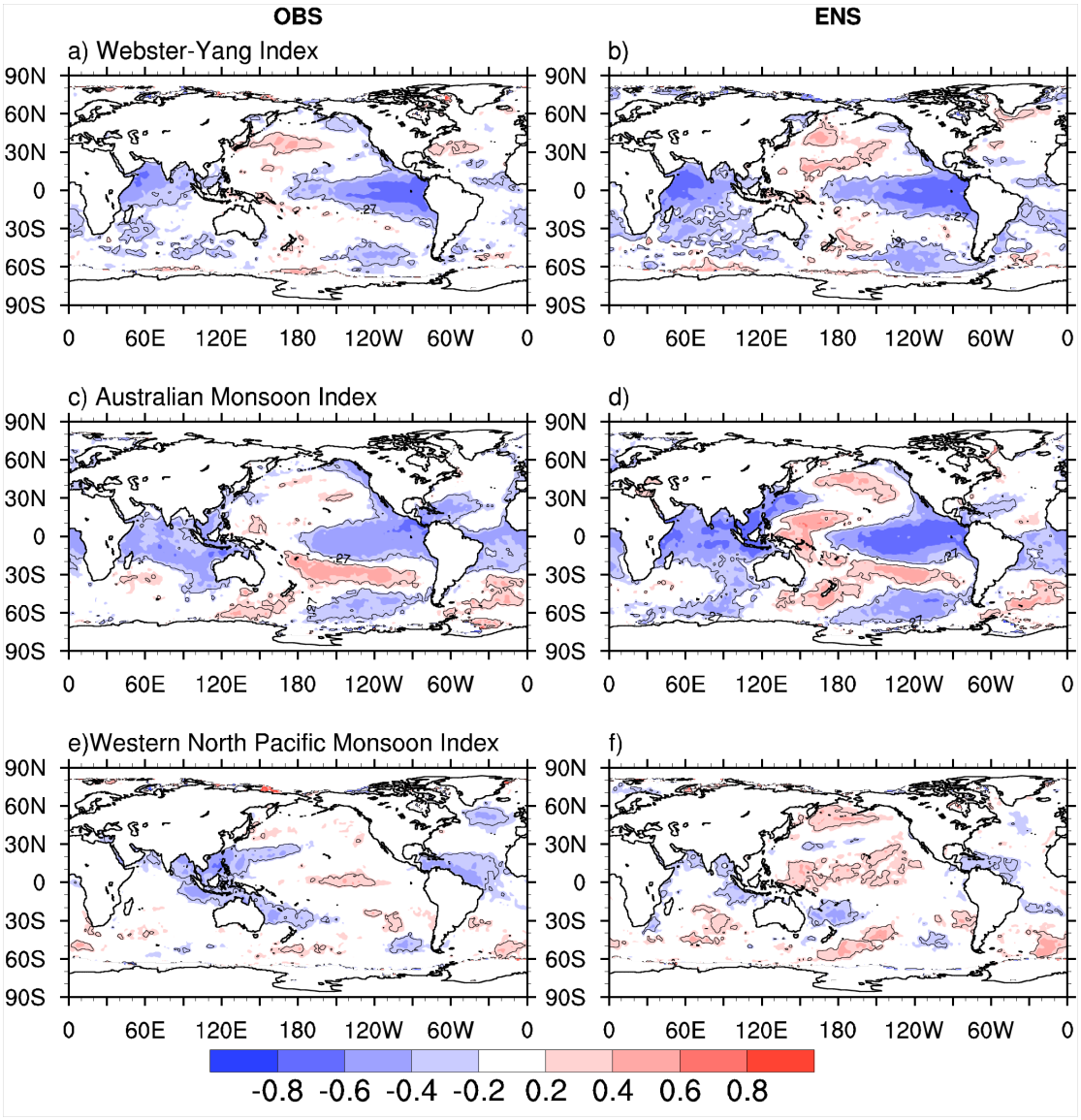

Figure 8 Spatial distributions of correlation coefficients between SSTs and Webster-Yang index (1st row), Australian monsoon index (2nd row), and western North Pacific monsoon index (3rd row) derived from the re-analysis (left column), and multi-model ensemble mean (right column). Only the correlations statistically significant at the 5% level are plotted.

Figure 9 Spatial distributions of correlation coefficients between previous winter (DJF) SSTs and western North Pacific summer monsoon index derived from (a) the re-analysis, and (b) multi-model ensemble mean. Only the correlations statistically significant at the 5% level are plotted. (c) Regression coefficients between normalized western North Pacific summer monsoon index and previous winter Nino 3 SST index (Unit 1/k). The regression coefficients statistically significant at the 5% level are shown as red dots. The correspondence of abscissa number with the model name is the same as Figure 7.

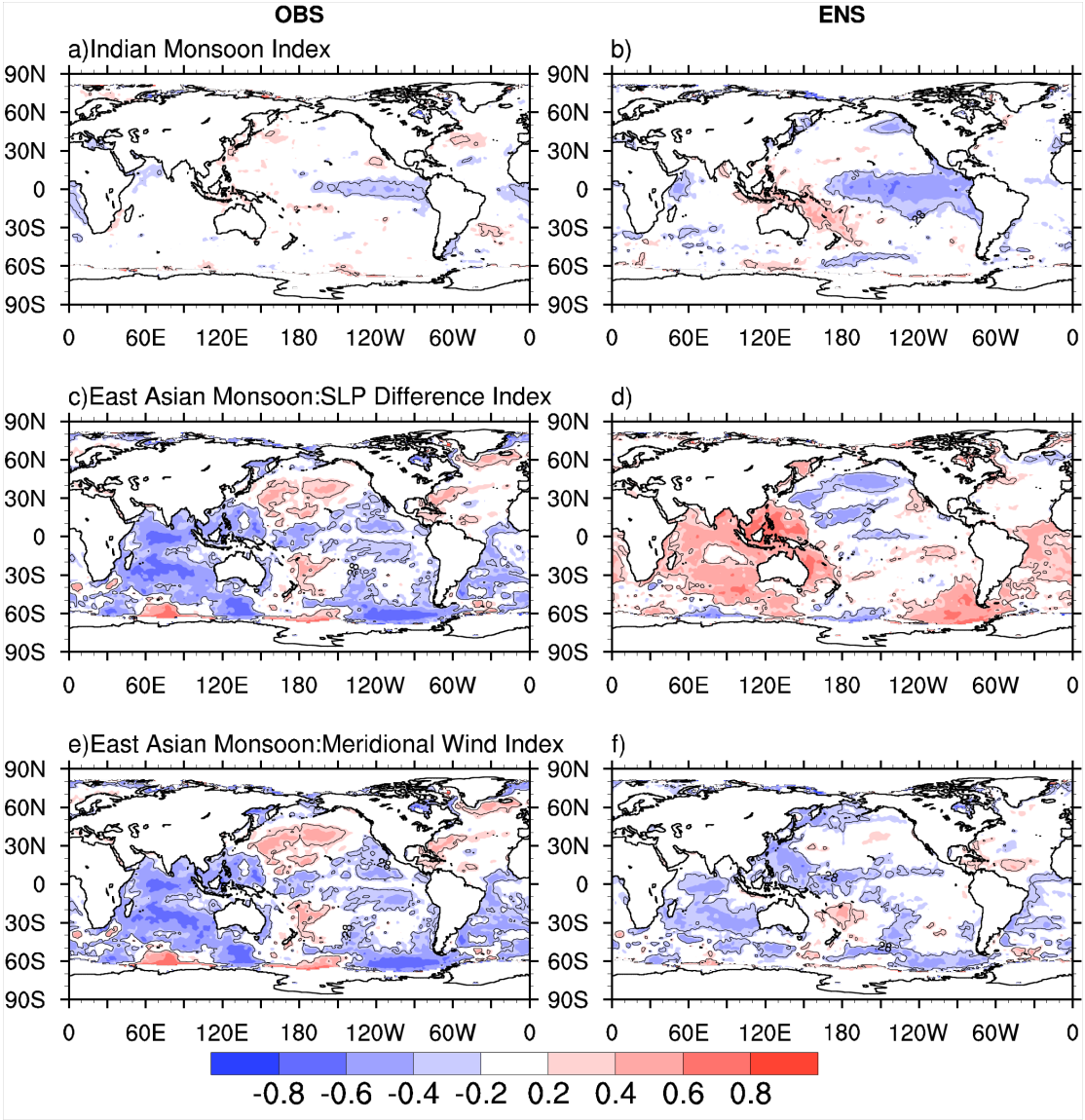

Figure 10 Same as **Figure 8** except for the Indian monsoon (1st row), East Asian monsoon SLP index (2nd row), and the East Asian monsoon meridional wind index (3rd row). Only the correlations statistically significant at the 5% level are plotted.

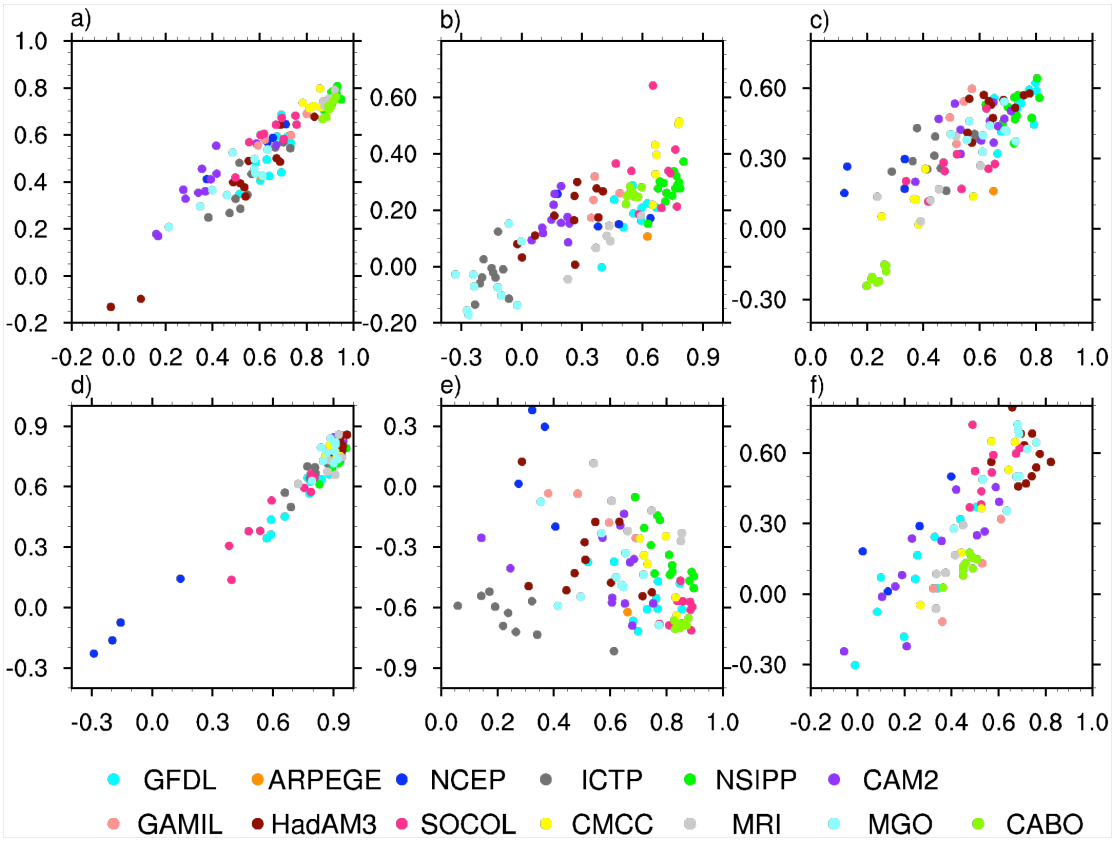

Figure 11 Pattern correlation coefficient of SST anomalies associated with observed and modeled monsoon indices. The abscissa (ordinate) represents pattern correlation coefficients of SST anomalies between the observation (MME) and each individual simulation. Each dot represents one realization. (a) Webster-Yang index, (b) Indian monsoon index, (c) Western North Pacific monsoon index, (d) Australian monsoon index (e) East Asian monsoon SLP index (f) East Asian monsoon meridional wind index.